Methods

Visual behavior tasks

Two alternative forced swim tasks were performed in a trapezoid shaped pool (sides a = 25 cm, b = 80 cm, c and d = 143 cm) with two side-by-side monitors (19 inches, V196L, Acer) placed at the wide end (b) of the tank and separated by a black divider (42 cm). Detailed instructions for the apparatus were described previously [1]. A rescue platform (37 cm ×13 cm × 14 cm) was hidden under water below the monitor with the positive visual cue (termed the S+ side). Visual cues (i.e. different grating pattern) were generated in the Gabor-patch generator (https://www.cogsci.nl/gabor-generator). The visual cue and hidden platform were moved to the right or left screens in a pseudorandom manner with the following orders: LRLLRLRLRR, RLRRLRLRLL, RRLRLLRLRL and LLRLRRLRLR. During the behavioral tasks the room was dark, but a 60 W bulb was positioned above the holding cages. During the visual tasks, mice were held in separate cages placed on to heating pads and lined with paper towels. A day before starting experiments, mice were acclimated to the experimenter and the pool through handling, a 1–2 min period of direct contact with the hidden platform at either arms, and submersion into the water at gradually-increasing distances from the hidden platform. Behavioral tasks included a training phase (8 days) and a testing phase (10–12 days). For training phases, mice were placed at the center of the narrow end and given one minute to find the platform for 8–10 trials per day. A trial was recorded as a correct choice if a mouse passed the choice line on the S+ side, while passing the choice line on the S- side was recorded as an incorrect choice. After arriving at the rescue platform, mice were placed back into their individual cages. When a mouse made an incorrect choice, it was placed back at the release chute to perform another trial immediately before going back to its home cage. After 8 days of training, mice learned to find the positive visual cue (i.e. vertical gratings) with a >80% accuracy. To test visual acuity and contrast sensitivity, we increased the spatial frequency and decreased the contrast of vertical gratings (i.e. the S+ cue), respectively. In the testing phase of the detection tasks, 10 trials of a given task (e.g. detection of vertical gratings with spatial frequency of 0.32 cpd versus a gray screen) were performed in 10 consecutive days (one per day). No more than nine animals were tested in a given session. Each mouse performed no more than 10 trials per day. A total of 10 $CASK^{+/+}$ and 11 $CASK^{+/-}$ were tested. Mice were 2-6 months old at the start of training.

Electroretinography

Three female $CASK^{(+/-)}$ mice and three wild type female mice were dark-adapted overnight and anesthetized under infrared illumination by ketamine/xylazine/acepromazine through intraperitoneal injection (94/5/1 mg/kg), and pupils were dilated with eye drops containing 1% tropicamide and 2.5% phenylephrine (Bausch & Lomb, Tampa, FL). Body temperature was maintained at 35~37 °C by 43.5 °C circulating water through a plastic heating coil wrapped around the animals. Stimulus-dependent transcorneal potential changes from both eyes were simultaneously recorded using the UTAS BigShot system (LKC Technologies, Gaithersburg, MD). A series of calibrated white flashes with intensities ranging from 0.0000025 to 250 Candela sec m^{-2} were used as stimuli [2]. The interstimulus interval was 3 sec for dimmer flashes and increased to 120 sec for brighter flashes to ensure proper dark adaptation. Responses from 5 to 15 independent measurements were averaged for analysis. Photopic recordings ensued immediately after scotopic recordings by exposing the animals to a white background light of 30 Candela m^{-2}

intensity for 10 min followed by flashes of 25 Candela sec m^{-2} in intensity and presented at 1 Hz in frequncy for 90 sec. Ensemble scotopic ERG b-wave amplitude vs. retinal illuminance (Fig. 1I) was fitted to a modified Naka-Rushton function: A(x)=[R*x/(x+A)] + [C*x/(x+B)], where R and C are rod- and cone-driven maximum response amplitudes (in µV), respectively, and A and B are half-saturating light intensities for rod- and cone-driven responses, respectively.

Plasmid and Point Mutagenesis

pEGFP-C3-CASK (rat) plasmid has been previously described [3]. Using Phusion polymerase (NEB), point mutation P673L was generated in the pEGFP-C3-CASK plasmid by Site-directed mutagenesis and sequenced in the Core Laboratory Facility in the Virginia Bioinformatics Institute at Virginia Tech.

Cell Culture and Imaging

Human embryonic kidney (HEK-293) cells (ATCC) were plated on 50 µg/ml poly-L-lysine (Sigma Aldrich Inc.)-coated coverslips (Fisherbrand, Inc.) in 24-well plates (JetBiofil) and maintained in DMEM (Hyclone) containing 10% fetal bovine serum (Hyclone) supplemented with 5 mg/ml penicillin-streptomycin (Hyclone). Cells at 80% confluency were transfected with 0.5 µg of GFP-$CASK^{WT}$ and GFP-$CASK^{P673L}$ DNA per well using calcium phosphate method. Twenty hours post-transfection, cells were washed twice with phosphate buffered saline (Sigma Inc.) and fixed for 15 minutes at room temperature using a 4% paraformaldehyde solution. Coverslips were mounted on microscope slides (Premiere) using Vectashield (Vector Laboratories Inc.) and visualized using confocal laser scanning microscopy (ZEISS Axio Examiner.Z1 LSM 710).

Molecular Dynamics Simulations and Analysis

The UCSF Chimera software package [4] was used for molecular visualization and editing. Molecular dynamics simulations were performed using the program GROMACS 5.1.3 [5] on a previously constructed homology model of CASK's PDZ-SH3-GuK (PSG) supradomain [6] and the corresponding P673L mutant, which was constructed using with Chimera's Rotamers tool to replace the native proline with leucine at the position analogous to 673 with a leucine rotamer from the Dunbrack backbone-dependent rotamer library with the highest probability. The AMBER99SB-ILDN force field [7] was used for all simulations. Structures were solvated with a three-point water model (SPC/E) in an explicit rhombic dodecahedron water box (solute box distance of 1.0 nm) under periodic boundary conditions, with charges neutralized by chloride ions. Structures were then minimized and 100 ps NVT and NPT equilibration simulations were performed as previously described [6]. An unrestrained 100 ns NPT molecular dynamics simulation was run after equilibration. Three trajectories initiated with different random seeds were generated for both the wildtype and $CASK^{P673L}$ structures.

After post-processing to correct for periodicity, trajectories were used to calculate root mean square deviation (RMSD) and radius of gyration (Rg) of the protein backbone from the starting structure at each time point using the GROMACS rms and gyrate command, respectively, and a Welch's two-sample t-test (chosen due to unequal variance as evaluated by Levene's test) was run in R to evaluate differences in Rg between $CASK^{WT}$ and $CASK^{P673L}$. The root mean square

fluctuation (RMSF) of all alpha carbons from each of the three trajectories was also calculated (GROMACS rmsf command). RMSF values were used to calculate B-factors for each residue, which were then averaged, using the equation: B-factor = $(8\prod^2/3)$ x $(RMSF)^2$. Average representative structures were selected based on a cluster analysis of the three concatenated molecular dynamics trajectories (excluding the first 25 ns of each trajectory) for the wildtype and P673L PSG structures, respectively, that was performed using the GROMACS cluster command with a 3Å cutoff employing the gromos algorithm [8]. Secondary structure prediction to evaluate helical propensity was performed by using GROMACS to call the dssp program [9]; DSSP output was then analyzed using a Python program [10].

Neurexin mediated cell recruitment assay

Human embryonic kidney (HEK-293) cells (ATCC) were plated on 50 µg/ml poly-L-lysine (Sigma Aldrich Inc.)-coated coverslips (Fisherbrand, Inc.) in 24-well plates (JetBiofil) and maintained in DMEM (Hyclone) containing 10% fetal bovine serum (Hyclone) supplemented with 5 mg/ml penicillin-streptomycin (Hyclone). Cells at 80% confluency were co-transfected with 0.5 µg of Flag tagged Neurexin1-β and GFP-$CASK^{WT}$ or GFP-$CASK^{P673L}$ DNA per well using calcium phosphate method. Twenty hours post-transfection, cells were washed twice with phosphate buffered saline (Sigma Inc.) and fixed for 15 minutes at room temperature using a 4% paraformaldehyde solution. Cells were permeabilized using PBS with 0.01% Triton-X 100 solution and blocked using 5% fetal bovine serum. Cells were immunostained using monoclonal anti-FLAG antibody (1:100) followed by Alexa-633(1:250) anti-mouse antibody. Similar to the mounting and imaging procedure described above.

Solubility assay

Human embryonic kidney (HEK-293) cells (ATCC) were plated in 6-well plates (JetBiofil) and maintained in DMEM (Hyclone) containing 10% fetal bovine serum (Hyclone) supplemented with 5 mg/ml penicillin-streptomycin (Hyclone). Cells at 80% confluency were transfected with 10 µg of EGFPN1, GFP-$CASK^{WT}$ or GFP-$CASK^{P673L}$ DNA per well using calcium phosphate method. Two days later cells were harvested and solubilized in RIPA buffer containing PBS, 1%Triton X-100, 0.5% sodium deoxycholate, 2mM EDTA, 1mM EGTA and protease inhibitors (0.1 mg/ml aprotinin, 0.1 mg/ml leupeptin, 0.1 mg/ml pepstatin, and 0.01 mg/ml PMSF; all purchased from Fisher Scientific). Pellets and supernatant were obtained after centrifuging lysates for 30 min. at 15,000 rpm at 4°C. Pellets and supernatants were boiled with SDS sample buffer, proteins were separated using SDS PAGE and blotted with CASK antibody.

Pull down assay using NXCT and GST beads

Human embryonic kidney (HEK-293) cells (ATCC) were plated in 6-well plates (JetBiofil) and maintained in DMEM (Hyclone) containing 10% fetal bovine serum (Hyclone) supplemented with 5 mg/ml penicillin-streptomycin (Hyclone). Cells at 80% confluency were transfected with 10 µg of EGFPN1, GFP-$CASK^{WT}$ or GFP-$CASK^{P673L}$ DNA per well using calcium phosphate method. Two days later cells were harvested and solubilized in RIPA buffer containing PBS,

1%Triton X-100, 0.5% sodium deoxycholate, 2mM EDTA, 1mM EGTA and protease inhibitors (0.1 mg/ml aprotinin, 0.1 mg/ml leupeptin, 0.1 mg/ml pepstatin, and 0.01 mg/ml PMSF; all purchased from Fisher Scientific). The lysates were incubated by rocking at 4°C for 30min and then centrifuged for 30 min. at 15,000 rpm at 4°C to collect the supernatants. The precleared supernatants were incubated with 30ul of GST (glutathione-s-transferase) and NxCT GST sepharose beads and incubated on rocker for 2hr 4°C. The beads were washed three times with PBS containing 1% Triton X 100 buffer. 30 µl of 2x SDS sample buffer was added to the beads and boiled 100C for 10min. Protein samples were separated using SDS-Page and immunoblotted for CASK.

Immunoblots

Proteins were resolved using SDS-PAGE (sample volumes loaded were based on estimates of appropriate protein concentration), transferred to a nitrocellulose membrane (Fisher), and immunoblotted for the proteins of interest. HRP-conjugated secondary antibody were used. The blots were developed using Amersham ECL western blotting detection reagents (GE Healthcare Life Sciences) for HRP secondaries. All blots were imaged using a ChemiDoc™ MP System (BioRad). Antibodies used are CASK (mouse monoclonal Ab, Cat. No. 75000, 1:1000; NeuroMab), Synaptophysin (polyclonal, Cat. No. 336A-76, 1:1000, Sigma), β-Actin (mouse monoclobal Ab, Cat. No. MABT825 clone 4C2 lot# Q2653600, 1:1000, Sigma).

Immunohistochemistry

Mice were anesthetized and perfused with PBS and then 4% paraformaldehyde (PFA). Brain and retina were dissected and postfixed in 4% PFA. Tissues were cryopreserved in 30% sucrose before embedding in tissue freezing medium (Electron Microscopy Studies, Hatfield, PA) and cryosectioned using Leica CM1850 Cryostat (Leica Biosystems, Wetzlar, Germany) to generate 16-µm thick tissue sections for brain. Sections or tissue were permeabilized and blocked with 0.25% Triton X-100 and 5% BSA in PBS. Immunostaining was performed using primary antibodies at an appropriate concentration followed by labeling with fluorophore conjugated secondary antibodies. Primary antibodies include: Melanopsin (rabbit polyclonal Ab generated by Dr. C.K. Chen), RNA-binding protein with multiple splicing (RBPMS; rabbit polyclonal Ab, Cat. No. 1830, 1:500; PhosphoSolution, Aurora, CO, USA), CASK (Mouse IgG1, 1:100, Clone K56A/50, UC Davis/NIH NeuroMab Facility, Davis, CA), SMI32 (Mouse IgG1, 1:1000, Covance, Princeton, NJ), NeuroTrace (1:300, Cat No. N21480, ThermoFisher, Waltham, MA). For IHC with anti-CASK antibodies tissues were fixed in 100% Methanol. Secondary antibodies include: Alexa Fluor 488 (goat anti-rabbit, Cat. No. A-11008, 1:1000; Invitrogen) and Alexa Fluor 555 (goat anti-mouse IgG, Cat. No. A32727, 1:1000; Thermo Scientific, Waltham, MA, USA). Sections were mounted with VectaShield containing 4′,6-diamidino-2-phenylindole (DAPI; Vector Laboratories, Burlingame, CA, USA) and were imaged using a Zeiss 700 or 710 laser scanning confocal microscope (Oberkochen, Germany).

Optic Nerve Samples Preparation for Transmission Electronic Microscopy (TEM)

Mice were anesthetized and perfused with PBS and then 0.1 sodium cacodylate (NaCa) buffer containing 2% glutaraldehyde/2% PFA [2G/2PF] pH 7.4. Optic nerves were dissected and immersed in NaCa buffer overnight and then put in 2% OSO_4 for 2 hours for postfixation. Dehydration was achieved by sequentially adding 15% to 100% ethanol. Samples were embedded in 100% epoxy resin and cured at 58°C. Sectioning of samples for TEM was performed at Virginia-Maryland College of Veterinary Medicine at Virginia Tech.

Axon Counts

Axons were counted on 4000X and 8000X TEM images using spyglass [11] virtual reality software and Oculus rift hardware (Best Buy). Images were uploaded into syGlass as TIFFs with voxel dimension of 1x1x1 nm. In spyglass, each image was optimized for quantification by reducing the stride and optimizing image intensity. The counting feature of syGlass was used to mark every axon in the field of view.

Optic Nerve Area

Toluidine blue images were imaged on a Zeiss AxioImager A2 fluorescent microscope at 20X objective. Images were uploaded to ImageJ and the freehand tool was used to circle the optic nerve.

RGC Counts

Cell counts were performed on 16-μm cryosectioned 4% PFA- fixed retinal tissue as described previously(Liang)8. Slides were stained with DAPI (diluted 1:5000 in PBS) for 60 seconds and then mounted with VectaShield (Vector Laboratories). Images of central retina were acquired on a Zeiss LSM 700 confocal microscope or a Zeiss Axio Imager A2 fluorescent microscope. All RBPMS-positive cells in the ganglion cell layer were counted manually under 320 objective. Cell counts were analyzed from at least four animals for each age and genotype. Five images per retina per mouse were analyzed.

G Ratio

G-ratio, defined as the ratio of inner axonal diameter to the outer axonal diameter (including myelin sheath), of 200 axons in the ON were measured on TEM images (×4000) using ImageJ software (http://imagej.nih.gov/ij/; provided in the public domain by the National Institutes of Health, Bethesda, MD, USA). The measurements of inner and outer axonal diameters (d) were calculated from inner and outer axonal areas (a), respectively, to reduce error because the sections were not perfectly round in shape, where $d \approx 2\sqrt{(a/\pi)}$.

Table1.Genotyping was done using a PCR-based method with following primer pairs

Gene	Forward	Reverse
Cask	TTTGGGGACTAGATGGGTGTGGTG	CTTGGTCGCAGCTTGGGAGTA
Cask-lox	GTCGCAGCTTGGGAGTAGAG	ACTAACCCTCCTCCCTTTCG

Cre	CGTACTGACGGTGGGAGAAT	TGCATGATCTCCGGTATTGA
tdT	ACCTGGTGGAGTTCAAGACCATCT	TTGATGACGGCCATGTTGTTGTCC

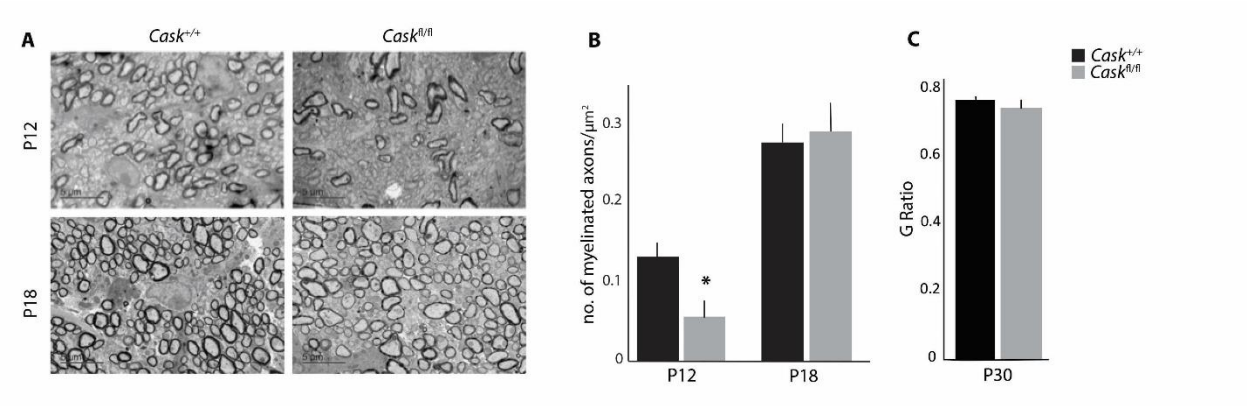

Supplemental Figure 1: Delay of myelination in Cask$^{fl/fl}$ RGC axons

(A) TEM of RGC axons in the ON in *Cask*$^{fl/fl}$ and wild-type controls at P12 and P18. Scale bar = 5 µm. (B) Quantification axon of density (per µm^2). (C) G-ratio measurements (i.e. myelin thickness divided by axon diameter) in age-matched mutants and controls. n=3 mice per genotype. * denotes $p < 0.05$ by two-way ANOVA. Data is plotted as mean±SEM.

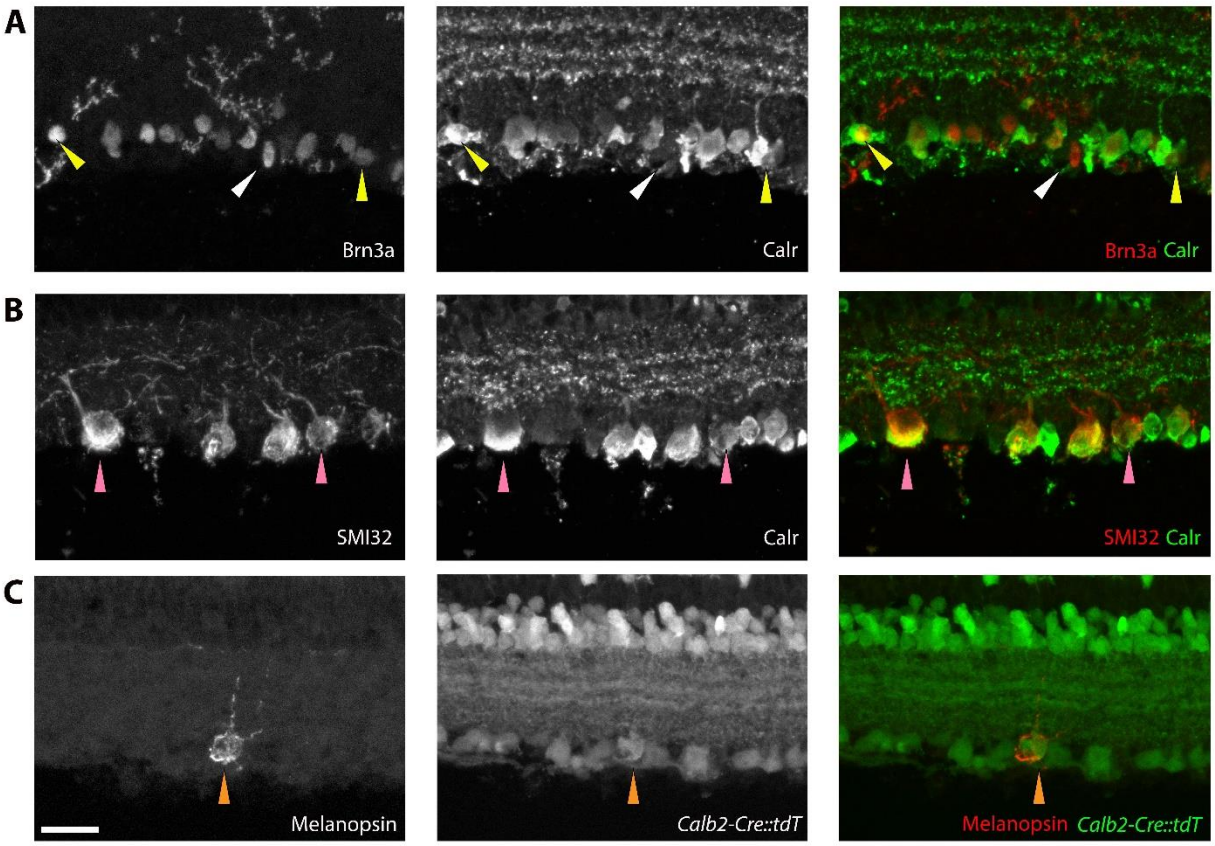

Supplemental Figure 2: Calretinin expression in RGC subtypes. (A) Co-localization of Calr and Brn3a. White arrows indicate Brn3a^{+}Calr^{-} cells. Yellow arrows indicate Brn3a^{+}Calr^{+} cells. (B) Co-localization of Calr and SMI32. Pink arrows indicate Brn3a^{+}SMI32^{+} cells. (C) Co-localization of Calr and Melanopsin. Orange arrows indicate Brn3a^{+}Melanopsin^{+} cells.

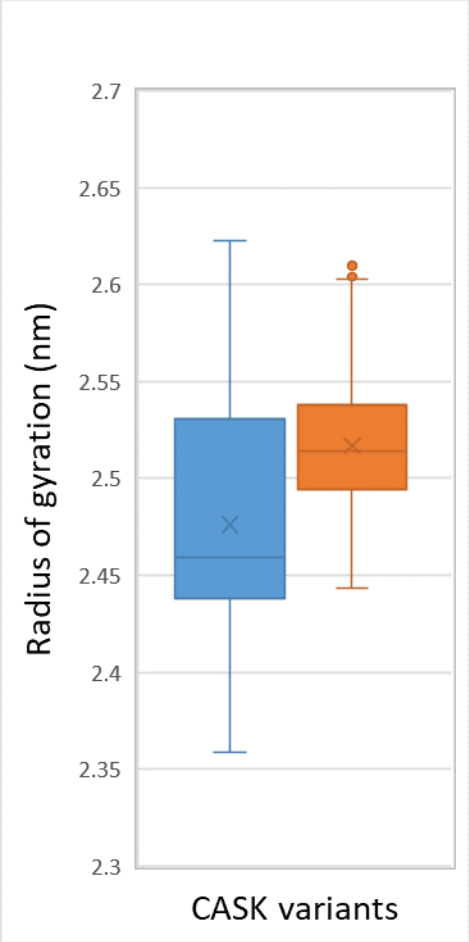

Supplemental Figure 3: CASK^{WT} PSG model adopts, on average, a more compact conformation than CASK^{P673L}. Box plots of the minimum, median (line), mean (x), and maximum radius of gyration (Rg) of the protein backbone calculated at each timepoint of the concatenated MD trajectories for the PSG structures of CASK^{WT} and CASK^{P673L}. The mean Rg's (CASK^{WT}, 2.48 nm; CASK^{P673L}, 2.51 nm) are statistically significantly different from each other based on a Welch's t-test, chosen due to the evident unequal variance, as confirmed using Levene's test.

References

1. Prusky GT, West PWR, Douglas RM. Behavioral assessment of visual acuity in mice and rats. *Vision Res* 2000;40:2201-2209.
2. Li S, Chen D, Sauve Y, McCandless J, Chen YJ, Chen CK. Rhodopsin-iCre transgenic mouse line for Cre-mediated rod-specific gene targeting. *Genesis* 2005;41:73-80.
3. Mukherjee K, Sharma M, Urlaub H, et al. CASK Functions as a Mg2+-independent neurexin kinase. *Cell* 2008;133:328-339.
4. Pettersen EF, Goddard TD, Huang CC, et al. UCSF Chimera--a visualization system for exploratory research and analysis. *J Comput Chem* 2004;25:1605-1612.
5. Abraham MJ, Murtola T, Schulz R, et al. GROMACS: High performance molecular simulations through multi-level parallelism from laptops to supercomputers. *SoftwareX* 2015;1–2:19-25.
6. LaConte LEW, Chavan V, DeLuca S, et al. An N-terminal heterozygous missense CASK mutation is associated with microcephaly and bilateral retinal dystrophy plus optic nerve atrophy. *American Journal of Medical Genetics Part A* 2019;179:94-103.
7. Lindorff-Larsen K, Piana S, Palmo K, et al. Improved side-chain torsion potentials for the Amber ff99SB protein force field. *Proteins* 2010;78:1950-1958.
8. Daura X, Antes I, van Gunsteren WF, Thiel W, Mark AE. The effect of motional averaging on the calculation of NMR-derived structural properties. *Proteins-Structure Function and Genetics* 1999;36:542-555.
9. Touw WG, Baakman C, Black J, et al. A series of PDB-related databanks for everyday needs. *Nucleic Acids Res* 2015;43:D364-D368.
10. Henriques JM. https://gist.github.com/jmhenriques/9a531bce9d5f549d53a5/.
11. Pidhorskyi SM, M; Jones, Q; Spirou, G; Doretto, Gi. syGlass: Interactive Exploration of Multidimensional Images Using Virtual Reality Head-mounted Displays. *arXivorg* 2018;arXiv:1804.08197.